Proceedings of the
44th IEEE Conference on Decision and Control, and
the European Control Conference 2005
Seville, Spain, December 12-15, 2005



# Pneumatic Three-axis Vibration Isolation System Using Negative Stiffness

Takeshi Mizuno, *Member, IEEE,* Masato Murashita, Masaya Takasaki, and Yuji Ishino

***Abstract*— A three-axis active vibration isolation system with pneumatic actuators for generating negative stiffness was developed. A control method of realizing a suspension with negative stiffness by the actuator was derived. It was implemented in the developed system where each actuator was controlled locally. It was demonstrated experimentally that the equalization of the amplitude of negative and positive stiffness enables the system to have zero compliance to direct disturbance.**

## I. INTRODUCTION

For microvibration isolation, high performance is required in suppressing the effects of direct disturbance in addition to isolation from ground vibration. In conventional passive-type vibration isolation systems, however, a trade-off between them is inevitable because higher stiffness of suspension is better for the former while lower stiffness is better for the latter.

Mizuno has proposed a unique approach to breaking through the trade-off [1],[2]. The proposed vibration isolation system uses a zero-power magnetic suspension system. Since the zero-power system behaves as if it has a negative stiffness, infinite stiffness against static disturbances on the isolation table can be achieved by combining it with a normal spring. It enables the system to have good characteristics in both reducing vibration transmitted from ground and suppressing direct vibration.

In zero-power magnetic suspension systems, however, the magnitude of negative stiffness is a function of the gap between the electromagnet and the suspended object. When the mass on the isolation table varies, therefore, the negative stiffness varies from the nominal value so that the stiffness against direct disturbance becomes lower [2].

In this paper, we propose to use a pneumatic actuator instead of an electromagnet for generating negative stiffness. It can keep the stiffness very high for a wider range of operation than the former system. In addition, pneumatic actuator can support a heavy table by increasing their effective area acted on by air.

This paper is organized as follows. First, the concept of the proposed vibration isolation system is briefly described. Second, a control method of realizing negative stiffness with a pneumatic actuator is clarified by a transfer function approach. Third, a fabricated three-axis active vibration isolation system using pneumatic actuators is described. Fourth, its performance to direct disturbance is estimated experimentally.

## II. CONCEPT OF VIBRATION ISOLATION SYSTEM

### A. Serial Connection of Two Springs

The aim of this section is to show that infinite stiffness can be realized by connecting a normal spring with a spring that has negative stiffness in series. When two springs with spring constants of $k_1$ and $k_2$ are connected in series, the total stiffness $k_c$ is given by

$$k_c = \frac{k_1 k_2}{k_1 + k_2} \tag{1}$$

This equation shows that the total stiffness becomes lower than that of each spring when normal springs are connected. However, if one of the springs has negative stiffness that satisfies

$$k_1 = -k_2 , \tag{2}$$

the resultant stiffness becomes infinite, that is

$$|k_c| = \infty . \tag{3}$$

This research applies this principle of achieving zero compliance to direct disturbance acting on the vibration isolation table.

Manuscript received February 27, 2005. This work was supported in part by a Grant-in-Aid for Scientific Research (B) from the Ministry of Education, Culture, Sports, Science and Technology of Japan, and a research grant from Suzuki Foundation.

Takeshi MIZUNO is with the Department of Mechanical Engineering, Saitama University, Shimo-Okubo 255, Saitama 338-8570 Japan (corresponding author to provide phone: +81-48-858-3455; fax: +81-48-858-3712; e-mail: mizar@mech.saitama-u.ac.jp).

Masato MURASHITA was with Saitama University, Saitama 338-8570 Japan. He is now with Suzuki Motor Corporation, Japan.

Masaya TAKASAKI is with the Department of Mechanical Engineering, Saitama University, Shimo-Okubo 255, Saitama 338-8570 Japan (e-mail: masaya@mech.saitama-u.ac.jp).

Yuji ISHINO is with the Department of Mechanical Engineering, Saitama University, Shimo-Okubo 255, Saitama 338-8570 Japan (e-mail: yishino@mech.saitama-u.ac.jp).

0-7803-9568-9/05/$20.00 ©2005 IEEE

### B. Configuration of Vibration Isolation System

Fig.1 shows the general configuration of the proposed mechanism [3]. A middle mass $m_1$ is connected to the base through a spring $k_1$ and a damper $c_1$ that work as a conventional vibration isolator; sufficient isolation from ground vibration is achieved by setting $k_1$ to be small. A linear actuator is attached to the middle mass. The actuator suspends and drives an isolation table.

The linear actuator is controlled for the suspension system to have negative stiffness. In the initial steady states shown in Fig.2a, the distance between the table $m$ and the base is kept to be $L$. When the mass of the table increases by $\Delta m$, the distance increases by $\Delta L$ as shown in Fig.2b. The displacement of the table is in the direction opposite to the added force $\Delta mg$ so that the static stiffness of the suspension is given by

$$-\frac{\Delta mg}{\Delta L}(\equiv -k_n)\,. \tag{4}$$

When the actuator is controlled in this way, the system shown by Fig.1 behaves as follows. When the isolation table $m_2$ is subject to downward force $f_0$, the table would move upwards by $f_0/k_n$ if the middle mass were fixed. Meanwhile, the middle mass moves downwards by $f_0/k_1$ because of the increase of the suspension force. When $k_1 = k_n$, the increase in the length of the actuator is cancelled by the downward displacement of the middle mass. Thus the isolation table is maintained at the same position as before so that the system has zero compliance to direct static disturbance.

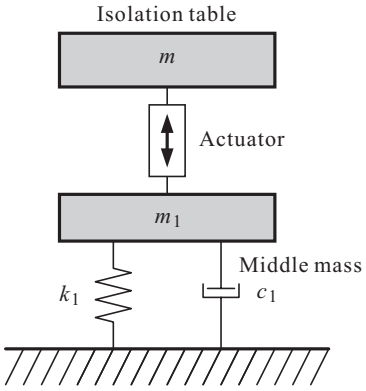


Fig. 1. General structure of the proposed vibration isolation system.

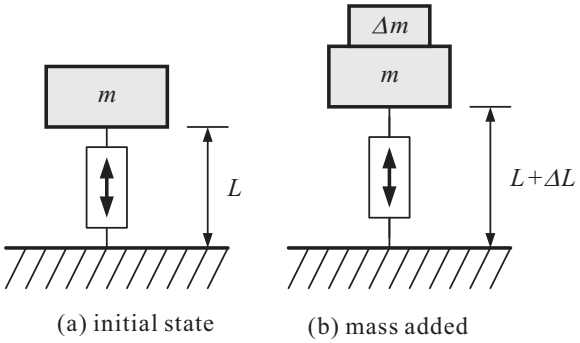


Fig. 2. Operation of the actuator

## III. Realization of Negative Stiffness

### A. Model

A pneumatic cylinder of diaphragm type is fabricated for the realization of suspension with negative stiffness. Fig.3 shows its schematic drawing. This type of cylinder is characterized by short stroke and small friction.

Fig.4 shows an analytical model for discussing the control system design. The cylinder moves a table $m$, which is connected to the base through a spring $k$ and a damper $c$. The equation of motion is given by

$$m\ddot{x} + c\dot{x} + kx = f_a + f_d\,, \tag{5}$$

where $f_a$ is the force generated by the cylinder, and $f_d$ is direct disturbance acting on the table. The force $f_a$ is given by

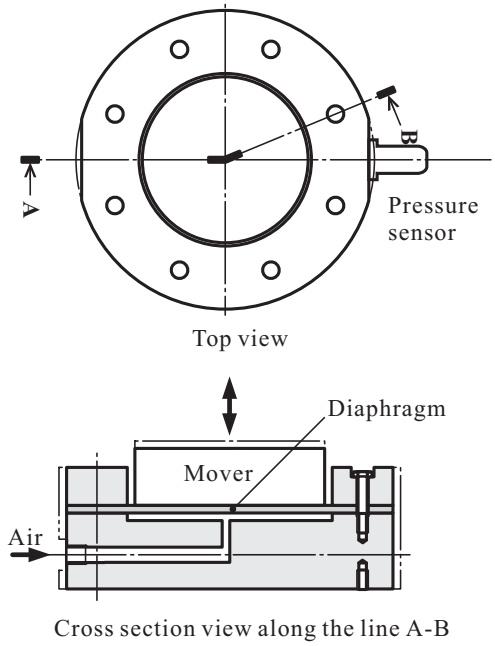


Fig. 3. Schematic drawing of pneumatic cylinder

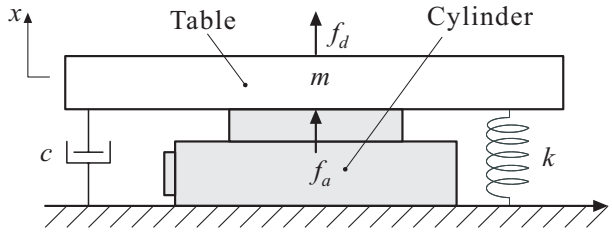


Fig. 4. Basic model

$$f_a = Ap\,, \tag{6}$$

where $A$ is the effective area of the cylinder, acted on by air, and $p$ is the pressure of the air. It is assumed that the pressure is controlled with a valve to satisfy

$$P(s) = \frac{k_i}{Ts+1} I(s)\,, \tag{7}$$

where $i$ is the coil current of the valve, $k_i$ is the pressure-current coefficient of the valve, and $T$ is the time constant depending on the dynamic characteristic. From (5) to (7), we get

$$X(s) = \frac{1}{t_o(s)}(b_0 I(s) + (d_1 s + d_0)F_d(s))\,, \tag{8}$$

where

$$t_o(s) = s^3 + a_2 s^2 + a_1 s + a_0\,,$$

$$a_2 = \frac{1}{T} + \frac{c}{m}\,, \qquad a_1 = \frac{k}{m} + \frac{c}{mT}\,, \qquad a_0 = \frac{k}{mT}\,,$$

$$b_0 = \frac{Ak_i}{mT}\,, \qquad d_1 = \frac{1}{m}\,, \qquad d_0 = \frac{1}{mT}\,.$$

*B. Control System Design*

The displacement of the table is treated as an output signal here. Considering linear output feedback control, we can represent the control input as

$$I(s) = -\frac{h(s)}{g(s)} X(s)\,. \tag{9}$$

When the transfer function of the controller is proper, the polynomials are represented as

$$g(s) = s^n + \sum_{k=0}^{n-1} g_k s^k\,, \tag{10}$$

$$h(s) = \sum_{k=0}^{n} h_k s^k\,. \tag{11}$$

Substituting (9) into (8) leads to

$$X(s) = \frac{g(s)}{t_o(s)g(s) + b_0 h(s)}(d_1 s + d_0)F_d(s)\,. \tag{12}$$

The disturbance is assumed to be stepwise so that it can be modeled as

$$F_d(s) = \frac{F_0}{s} \qquad (F_0 : \text{const}). \tag{13}$$

It is assumed that the controller is selected to stabilize the closed loop system. The steady-state displacement $x(\infty)$ is given by

$$\frac{x(\infty)}{F_0} = \lim_{s\to 0} \frac{(d_1 s + d_0)g(s)}{(s^3 + a_2 s^2 + a_1 s + a_0)g(s) + b_0 h(s)} = \frac{d_0 g_0}{a_0 g_0 + b_0 h_0}\,. \tag{14}$$

For the system to have negative stiffness with a magnitude of $k_n$, the following equation must be satisfied

$$\frac{d_0 g_0}{a_0 g_0 + b_0 h_0} = -\frac{1}{k_n}\,. \tag{15}$$

For assigning the closed-loop poles arbitrarily, third- or higher-order compensators are necessary. When a third-order compensator is used, the characteristic polynomial of the closed-loop system becomes

$$\begin{aligned} t_c(s) = {} & s^6 + (g_2 + a_2)s^5 + (g_1 + a_2 g_2 + a_1)s^4 \\ & + (g_0 + a_2 g_1 + a_1 g_2 + a_0 + b_0 h_3)s^3 \\ & + (a_2 g_0 + a_1 g_1 + a_0 g_2 + b_0 h_2)s^2 \\ & + (a_1 g_0 + a_0 g_1 + h_1 b_0)s + (a_0 g_0 + b_0 h_0) \end{aligned} \tag{16}$$

To obtain a system with a characteristic equation of the form

$$\begin{aligned} t_d(s) &= \prod_{n=1}^{3} (s^2 + 2\zeta_n \omega_n s + {\omega_n}^2) \\ &= s^6 + c_5 s^5 + c_4 s^4 + c_s s^3 + c_2 s^2 + c_1 s + c_0\,, \end{aligned} \tag{17}$$

we can match the coefficients to obtain

$$g_0 = -\frac{c_0}{d_0 k_n}\,, \tag{18}$$

$$g_1 = c_4 - a_1 - a_2 g_2\,, \tag{19}$$

$$g_2 = c_5 - a_2\,, \tag{20}$$

$$h_0 = \frac{1}{b_0}(c_0 - a_0 g_0)\,, \tag{21}$$

$$h_1 = \frac{1}{b_0}(c_1 - a_0 g_1 - a_1 g_0)\,. \tag{22}$$

$$h_2 = \frac{1}{b_0}(c_2 - a_0 g_2 - a_1 g_1 - a_2 g_0) \tag{23}$$

$$h_3 = \frac{1}{b_0}(c_3 - a_0 - a_1 g_2 - a_2 g_1 - g_0) \tag{24}$$

## IV. THREE-AXIS VIBRATION ISOLATION SYSTEM

*A. Experimental Apparatus*

Fig.5 shows a photograph of the fabricated cylinder. It has a diaphragm made of rubber with a thickness of 2 mm. Its

effective sectional area is approximately 50cm$^2$.

A photograph of a manufactured experimental apparatus with six cylinders is shown by Fig.6. Its schematic diagram is presented by Fig.7. The diameter and height is 200mm and 600mm, respectively. It has a circular isolation table and a circular middle table corresponding to the middle mass in Fig.2. The isolation and middle tables weigh 65kg and 75kg, respectively.

The middle table is suspended by three cylinders for positive stiffness and damping, which correspond to $k$ and $c$ in Fig.2. They are located at the vertices of an equilateral triangle on the base. The isolation table is suspended by three cylinders for negative stiffness, which are fixed to the middle table. Each cylinder for negative stiffness is aligned with a cylinder for positive stiffness vertically. Hence, the three-degree-of-freedom motions of the isolation table can be controlled by the proposed method. They are one translational motion in the vertical direction ($z$) and two rotational motions, pitch ( $\xi$ ) and roll ( $\eta$ ).

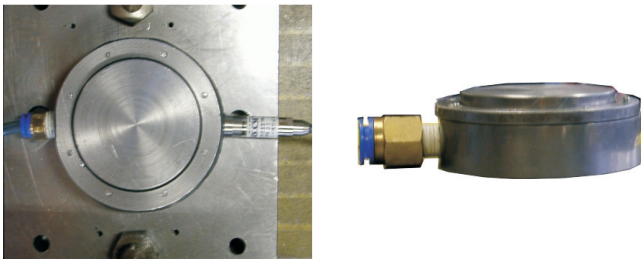

Fig. 5. Photograph of the cylinder

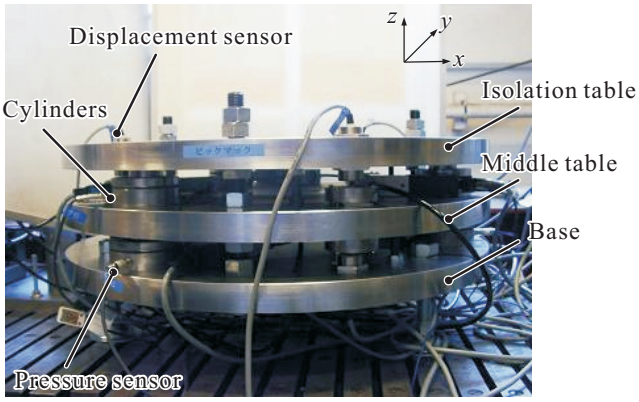


Fig. 6. Photograph of the experimental apparatus

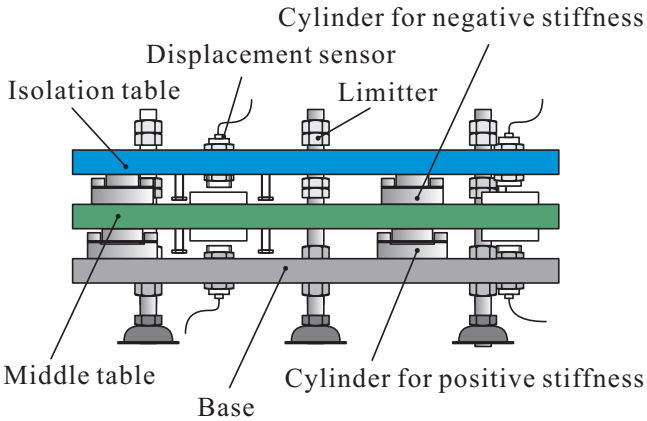


Fig. 7. Schematic drawing of the experimental apparatus

The displacements of the isolation table are detected by three eddy-current sensors, which located at the vertices of an equilateral triangle on the base. The displacement of the middle table is detected similarly. The detected places are shown in Fig.8, which are at the middle between the actuation positions (*not collocated*). The displacement at the position of each cylinder, and the displacement of each motion are calculated from these detected signals.

### *B. Structure of Controller*

For multi-channel control systems, there are two approaches to constructing the controller:

- local control (decentralized control)
- mode control (centralized control).

In the first controller, each actuator is controlled based on the local information, which is the displacement at the position in this case [4]. In the second controller, a compensator is built for each mode [5]. This work adopts the first approach. Each cylinder is controlled with a third-order controller whose coefficients are determined according to (18) to (24).

The control algorithm is implemented with a DSP-based digital controller. The control period is 100μs.

## V. Experimental Results

### *A. System Identification*

The parameters of the controlled object are estimated on the basis of frequency analysis. In the identification, three cylinders for negative stiffness are operated when the middle

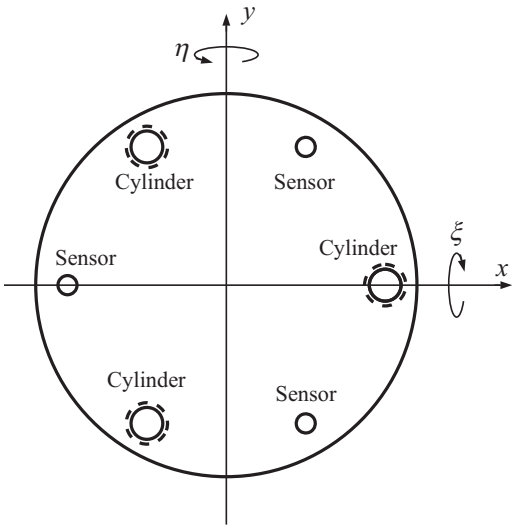


Fig. 8. Location of cylinders and sensors.

table is clamped not to move. It is assumed that the cylinders and control valves for controlling them are identical. They are driven simultaneously according to the same excitation signal so as to operate as a single cylinder that moves the isolation table in the *z*-direction. Parameter estimation is carried out for this virtual single cylinder.

Fig.9 show the frequency responses in which the output signal is (a) the displacement of the table, and (b) the pressure of the cylinder while the input signal is the excitation. They are approximated by third-order and first-order transfer functions, which are determined by using a curve-fitting program. The parameters of the controlled object are calculated from these transfer function.

### *B. Realization of Suspension with Negative Stiffness*

Suspension with prescribed negative stiffness is realized by the three cylinders. In this experiment, the middle mass is clamped not to move. Each cylinder is controlled to have the amplitude of negative stiffness to be

(a) $k_n = 250\,[\mathrm{kN/m}]$, (b) $k_n = 500\,[\mathrm{kN/m}]$.

The amplitude of stiffness in the *z*-direction is, therefore, set to be

(a) $k_n^z = 750\,[\mathrm{kN/m}]$, (b) $k_n^z = 1500\,[\mathrm{kN/m}]$.

The measured force-displacement characteristics are shown in Fig.10 in which force and displacement in the downward direction are represented to be positive, and vice versa. Disturbance force is produced by putting weights on the isolation table. It shows that the force-displacement relation is quite linear. The estimated stiffness is

(a) $\tilde{k}_n^z = 741\,[\mathrm{kN/m}]$, (b) $\tilde{k}_n^z = 1622\,[\mathrm{kN/m}]$.

The differences between the prescribed and experimental values are within 10%.

Fig.11 shows responses to stepwise disturbance in the *z*-direction. The poles are selected as

(a) $\omega_n = 2\pi\times 8\,[1/\mathrm{s}]$, $\varsigma_n = 0.8$ $(n = 1,\cdots,3)$,
(b) $\omega_n = 2\pi\times 10\,[1/\mathrm{s}]$, $\varsigma_n = 0.8$ $(n = 1,\cdots,3)$,
(c) $\omega_n = 2\pi\times 12\,[1/\mathrm{s}]$, $\varsigma_n = 0.8$ $(n = 1,\cdots,3)$.

The disturbance was generated by superimposing a rectangular signal on control signal. It demonstrates that the settling time can be reduced by setting $\omega_n$ to be large.

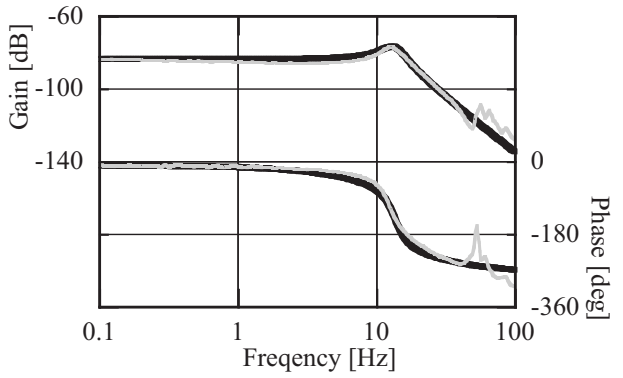


(a) Displacement characteristics

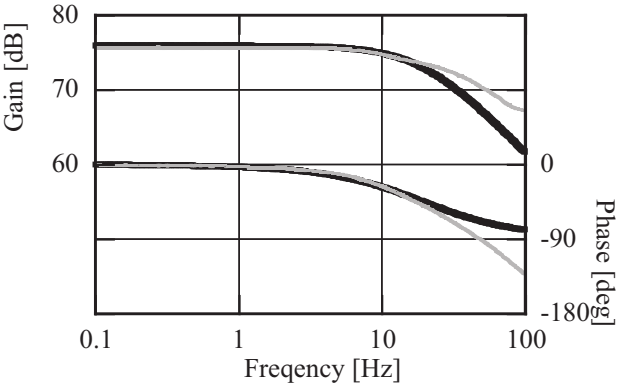


(b) Pressure characteristics

Fig.9. Frequency response of the cylinder
(Fine lines: measured results, Bold lines: approximating curves)

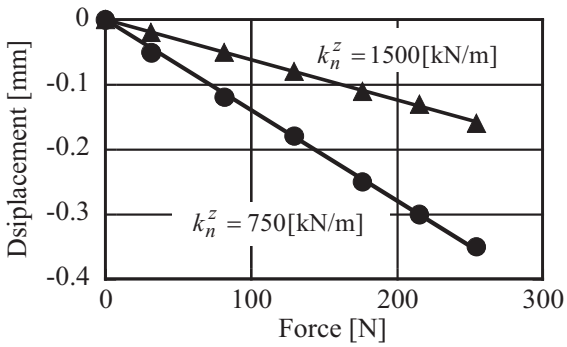


Fig.10. Realization of suspension with negative stiffness

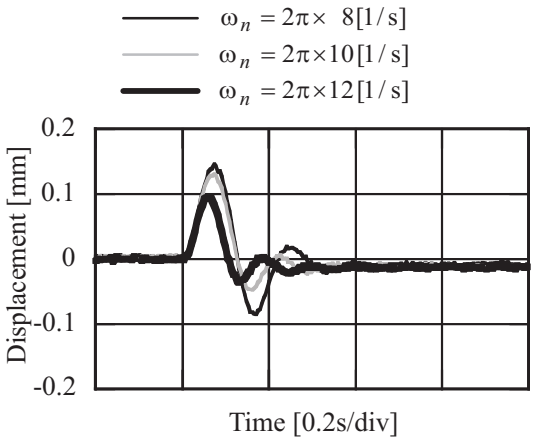


Fig.11. Responses to stepwise disturbance

### C. Realization of Suspension with Zero Compliance

In this experiment, the clamp of the middle table is released. Each cylinder suspending the middle table from the base is controlled to realize prescribed positive stiffness. Identification and control design for this cylinder are carried out in a manner similar to that described in the previous section. The difference is that (14) is replaced by

$$\frac{d_0 g_0}{a_0 g_0 + b_0 h_0} = \frac{1}{k_p}. \tag{24}$$

Fig.12 shows the displacement of the isolation table to the base, that of the isolation table to the middle mass and that of the middle mass to the base of the three modes. Each cylinder is controlled to have static stiffness of ±250 [kN/m]. It is observed that the position of the isolation table is maintained at the same position while the position of the middle mass changes proportion to direct disturbance in all the modes. The ratio of the total stiffness to the individual stiffness is

(a) 68 (translation)

(b) 12 (pitch)

(c) 12 (yaw)

This result demonstrates that the equalization of the amplitude of negative and positive stiffness enables the system to have virtually zero compliance to direct disturbance.

## VI. Conclusion

A three-axis active vibration isolation system with pneumatic actuators was developed. A control law for realizing a suspension with negative stiffness by using the pneumatic actuator was derived. Virtually zero compliance was achieved in the three modes by equalizing the amplitude of negative and positive stiffness individually.

Further study on vibration isolation characteristics to ground vibration is under way for the industrialization of the proposed vibration isolation system.

## References


[1] Mizuno, T., Proposal of a Vibration Isolation System Using Zero-power Magnetic Suspension, *Proc. Asia-Pacific Vibration Conference 2001*, Vol.2, pp.423-427, 2001.

[2] Mizuno, T., Vibration Isolation System Using Zero-Power Magnetic Suspension, *Preprints of 15th World Congress IFAC*, 955, 2002.

[3] Mizuno, T., Toumiya, T. and Takasaki, M., Vibration Isolation System Using Negative Stiffness, *JSME International Journal*, Series C, Vol.46, No.3, pp.807-812, 2003.

[4] Mizuno, T., Takasaki, M., Suzuki, H. and Ishino, Y., Development of a Three-Axis Active Vibration Isolation System Using Zero-Power Magnetic Suspension, *Proc. 42nd IEEE Conference on Decision and Control*, pp.4493-4498, 2003.

[5] Hoque, M.E., Takasaki, M., Ishino, Y. and Mizuno, T., Design of a Mode-Based Controller for 3-DOF Vibration Isolation System, *Proc. 2004 IEEE Conference on Robotics, Automation and Mechatronics*, pp.478-483, 2004.


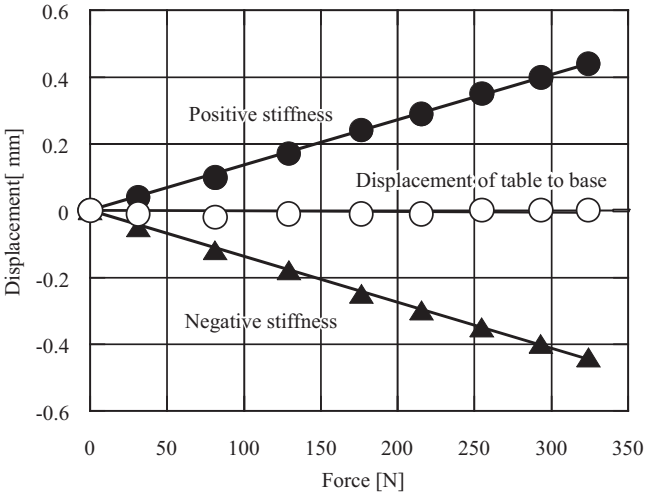


(a) Translation ($z$)

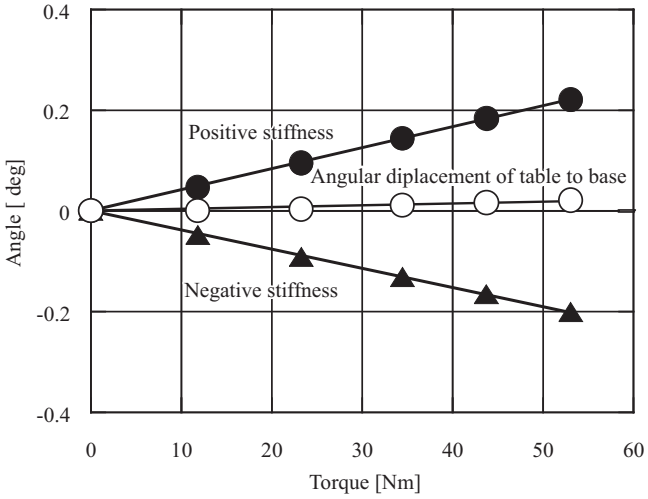


(b) pitch ( $\xi$ )

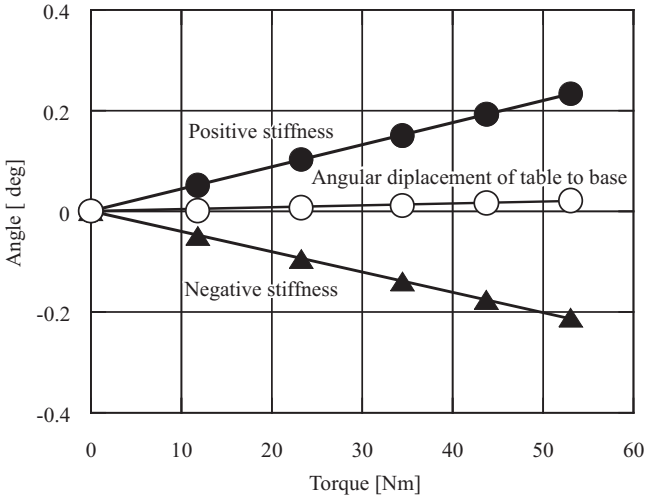


(c) roll ( $\eta$ )

Fig.12. Force-displacement characteristics of the isolation system